

AD-A044 168

NATIONAL BUREAU OF STANDARDS WASHINGTON D C  
EVIDENCE FOR THE CONFORMATION OF H2O ADSORBED ON RU(001).(U)  
JUL 77 T E MADEY, J T YATES

F/6 7/4

UNCLASSIFIED

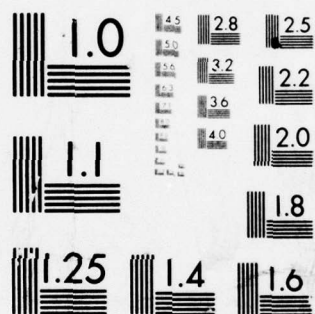
TR-5

N00014-77-F-0012

NL

| OF |  
AD  
A044 168





MICROCOPY RESOLUTION TEST CHART  
NATIONAL BUREAU OF STANDARDS-1963-A

AD A 044 168

OFFICE OF NAVAL RESEARCH  
Contract N00014-77-F-0012

① 2

Technical Report  
Evidence for the Conformation of  $H_2O$   
Adsorbed on Ru(001)

by

Theodore E. Madey and John T. Yates, Jr.  
Surface Processes and Catalysis Section  
National Bureau of Standards  
Washington, DC 20234

DDC  
REPRODUCED  
SEP 14 1977  
C

15 July 1977

Reproduction in whole or in part is permitted for  
any purpose of the United States Government

Approved for Public Release; Distribution Unlimited

To be published in Chemical Physics Letters

AD No. \_\_\_\_\_  
DDC FILE COPY

UNCLASSIFIED

SECURITY CLASSIFICATION OF THIS PAGE (When Data Entered)

REPORT DOCUMENTATION PAGE		READ INSTRUCTIONS BEFORE COMPLETING FORM
1. REPORT NUMBER Report # 5	2. GOVT ACCESSION NO.	3. RECIPIENT'S CATALOG NUMBER 9
4. TITLE (and Subtitle) Evidence for the Conformation of $H_2O$ Adsorbed on Ru(001).		5. TYPE OF REPORT & PERIOD COVERED Interim Report.
		6. PERFORMING ORG. REPORT NUMBER
7. AUTHOR(s) Theodore E. Madey and John T. Yates, Jr.		8. CONTRACT OR GRANT NUMBER(s) N00014-77-F-0012
9. PERFORMING ORGANIZATION NAME AND ADDRESS Surface Processes and Catalysis Section National Bureau of Standards Washington, DC 20234		10. PROGRAM ELEMENT, PROJECT, TASK AREA & WORK UNIT NUMBERS
11. CONTROLLING OFFICE NAME AND ADDRESS Office of Naval Research Physics Program Office Arlington, VA 22217		12. REPORT DATE 15 July 1977
14. MONITORING AGENCY NAME & ADDRESS (if different from Controlling Office) TR-5		13. NUMBER OF PAGES 22 p.
		15. SECURITY CLASS. (of this report) Unclassified
		15a. DECLASSIFICATION/DOWNGRADING SCHEDULE
16. DISTRIBUTION STATEMENT (of this Report) Approved for Public Release; Distribution Unlimited		
17. DISTRIBUTION STATEMENT (of the abstract entered in Block 20, if different from Report)		
18. SUPPLEMENTARY NOTES		
19. KEY WORDS (Continue on reverse side if necessary and identify by block number) Electron stimulated desorption, thermal desorption spectroscopy, water, ruthenium, surface, chemisorption.		
20. ABSTRACT (Continue on reverse side if necessary and identify by block number) The Electron Stimulated Desorption Ion Angular Distributions (ESDIAD) method has been used to study the adsorption of $H_2O$ by Ru(001). The results indicate that chemisorbed, undissociated $H_2O$ is bonded to Ru via the oxygen atom, and that interactions between neighboring molecules occur as coverage increases. The utility of ESDIAD for structure determination in the absence of long range order is demonstrated.		

DD FORM 1 JAN 73 1473

EDITION OF 1 NOV 65 IS OBSOLETE  
S/N 0102-014-6601

UNCLASSIFIED

SECURITY CLASSIFICATION OF THIS PAGE (When Data Entered)

240800





EVIDENCE FOR THE CONFORMATION OF  $H_2O$  ADSORBED ON Ru(001)

Theodore E. Madey and John T. Yates, Jr.  
Surface Processes and Catalysis Section  
National Bureau of Standards  
Washington, DC 20234

ABSTRACT

The Electron Stimulated Desorption Ion Angular Distributions (ESDIAD) method has been used to study the adsorption of  $H_2O$  by Ru(001). The results indicate that chemisorbed, undissociated  $H_2O$  is bonded to Ru via the oxygen atom, and that interactions between neighboring molecules occur as coverage increases. The utility of ESDIAD for structure determination in the absence of long range order is demonstrated.

Section <input checked="" type="checkbox"/>	
B. H. Section <input type="checkbox"/>	
<input type="checkbox"/>	
BY	
DISTRIBUTION/ANAL. ACTIVITY CODES	
Dis	SPECIAL
A	

## I. INTRODUCTION

A central problem in the physics and chemistry of surfaces concerns the determination of bonding geometry for atoms and molecules at surfaces. It has been shown recently that the method of Electron Stimulated Desorption Ion Angular Distributions (ESDIAD) has potential for the determination of the binding sites and bonding conformations of adsorbed species.<sup>(1,2)</sup> When an adsorbed layer is bombarded by a focussed beam of low energy electrons ( $\sim 100$  eV), the desorption of positive ions, ground state neutrals, and metastable species can be induced by electron excitation of the adsorbate. The positive ions liberated as a result of electron stimulated desorption have been observed to desorb in discrete "cones" of emission, in symmetric patterns having the symmetry of the substrate. The desorption of ions in narrow cones of emission is related to the formation of localized bonds at the surface.

A key question concerning the utility of ESDIAD for the study of surface structures concerns the relation between the directionality of surface bonds and the angle of ion emission. In order to examine the question experimentally, we are studying the adsorption of physisorbed and weakly chemisorbed molecules such as  $\text{H}_2\text{O}$ ,  $\text{NH}_3$ ,  $\text{C}_3\text{H}_6$ ,  $\text{C}_6\text{H}_{12}$  and  $\text{C}_8\text{H}_{16}$  on a close packed Ru(001) substrate. The objective is to see if the non-dissociative adsorption of a molecule having known geometry results in the appearance of an ESDIAD pattern whose symmetry and ion desorption angles are consistent with this known adsorbate geometry. The present report is concerned with ESDIAD studies of  $\text{H}_2\text{O}$  adsorbed on Ru(001).

On the basis of the molecular orbital structure of the free  $\text{H}_2\text{O}$  molecule,<sup>(3,4)</sup> it was expected that the initial interaction with a metal surface would be via the non bonding, or "lone pair" electrons on the O atom. It was thus

anticipated that the molecule would be bound to the surface through the oxygen atom, with the hydrogen atoms directed away from the surface. The experimental ESDIAD results substantiate the picture, and provide new insights into surface bonding configurations.

## II. EXPERIMENTAL

The apparatus used for these studies has been described in detail previously.<sup>(1)</sup> The single crystal Ru(001) sample was mounted on an XYZ-rotary manipulator. The sample temperature range was controlled by resistive heating in the range 80 K to 1550 K; temperatures were measured via a W-3% Re/W-26% Re thermocouple spot-welded to the crystal. The sample was cleaned by repeated heating between 300 K and 1550 K in O<sub>2</sub> at  $5 \times 10^{-7}$  Torr, a procedure which has been previously demonstrated using Auger electron spectroscopy<sup>(5)</sup> to produce a Ru surface free of S and C. The oxygen was removed by heating in vacuo to 1550 K, after which a sharp (1 x 1) LEED pattern characteristic of the clean Ru(001) surface was observed. The effectiveness of the surface cleaning procedure was verified at the end of these experiments by installation of an Auger spectrometer in the experimental chamber.

The maximum electron beam current in these studies was  $1.5 \times 10^{-7}$  A (current density  $\sim 2 \times 10^{-5}$  A/cm<sup>2</sup>). The weak positive ion desorption signals were detected using a hemispherical grid assembly backed by a double micro-channel plate (MCP) detector. The ESDIAD patterns were displayed visually by acceleration of the output electrons from the MCP detector onto a fluorescent screen. By reversing potentials, the low energy electron diffraction (LEED) pattern from the surface could also be displayed. A quadrupole mass spectrometer (QMS) was used for residual gas analysis, as well as for mass analysis of positive ions produced by electron impact on the



adsorbed layer. Use of a molecular beam gas doser insured that the  $H_2O$  flux directed onto the sample during adsorption was considerably higher than the background flux of residual gases in the vacuum chamber.

Typical electron excitation energies for the ESD studies were in the range 100 to 200 eV: typical electron energies for the LEED measurements were 90 to 200 eV. The angle of incidence of the electron beam for most ESD and LEED measurements was  $50^\circ$  with respect to the crystal normal.

### III. RESULTS

#### A. Electron Stimulated Desorption

Fig. 1a shows a LEED pattern from the clean Ru(001) substrate. When the Ru(001) crystal at  $\sim 90$  K was dosed with  $H_2O$  to a coverage  $< 0.2$  monolayers (as determined by thermal desorption spectroscopy, (see below)), the ESDIAD pattern of Fig. 1b resulted. The pattern is quite dim and has a characteristic "halo" with a dark area in the center indicating that  $H^+$  ion desorption normal to the surface was negligible. When the  $H_2O$  coverage was increased to more than 0.2 monolayers, a hexagonal array of emission cones was seen (Fig. 1c). As can be seen by comparing Fig. 1a and 1c, the azimuthal orientation of the  $H^+$  hexagon differs from the azimuthal orientation of the Ru(001) LEED pattern (which is based on the reciprocal lattice). However, in real space, the  $H^+$  ESDIAD hexagon and the hexagonal array of substrate atoms have the same orientation. In some cases, the hexagonal  $H^+$  array appeared to be superimposed upon the "halo" patterns; in other cases, the contrast between cones was higher. In general, there was evidence of increased emission in a direction about the normal to the surface. (The decrease of pattern intensity from upper left to lower right in the pictures is apparently a result of a spatial variation in gain of the imaging system).

The species yielding patterns of Fig. 1b and 1c were susceptible to electron beam damage. Changes in intensity were generally apparent after times of the order of 10 seconds at a current density of  $2 \times 10^{-5} A/cm^2$  at 200 V.

When a sufficiently high dose of  $\text{H}_2\text{O}$  vapor onto the 90 K surface resulted in the formation of an ice multilayer, the pattern of Fig. 1d developed. This intense pattern was dominated by emission normal to the surface.

Mass analysis of the ESD ions using the QMS indicated that for all the patterns of Fig. 1, the dominant ionic species detected was  $\text{H}^+$ . Small quantities of  $\text{O}^+$  ( $< 10\%$ ) were seen from submonolayer deposits of  $\text{H}_2\text{O}$  following short periods of electron bombardment during which time the ESDIAD patterns changed. Traces of ions at mass 2 and in the mass 16 to 19 range were seen for ESD of the ice multilayer and were identified as  $\text{H}_2^+$ ,  $\text{O}^+$ ,  $\text{OH}^+$ ,  $\text{H}_2\text{O}^+$  and  $(\text{H}_2\text{O})\text{H}^+$ . The intensities of each of these product ions from the multilayer was small, typically  $< 1\%$  of the dominant  $\text{H}^+$  emission. The maximum kinetic energy of  $\text{H}^+$  ions from the  $\text{H}_2\text{O}$  multilayer was determined using a retarding potential to be 13 eV (uncorrected for work functions).

The angle between the surface normal and the ring of maximum intensity in the ESDIAD "halo" of Fig. 1a was estimated by observing the angle through which the manipulator had to be rotated in order to center the region of maximum intensity (determined visually) on the optical axis of the ion detection system. Data showing the apparent value of the  $\text{H}^+$  emission cone half-angle  $\alpha$  are plotted in Fig. 2 as a function of the potential  $V_B$  applied between the crystal and the first hemispherical grid in the detection system.<sup>(1)</sup> A least squares extrapolation of these data to field-free conditions ( $V_B=0$ ) yields a value of  $\alpha = 58 \pm 5^\circ$ . Uncertainties in this measurement arise from the low intensity of the  $\text{H}^+$  emission, the rapid decay of intensity with time, and the distortion of the  $\text{H}^+$  ion pattern



due to the field between crystal and grid. The cone angle of  $H^+$  emission is  $116 \pm 10^\circ$  in comparison with the HOH angle of  $104.5^\circ$  in the free water molecule. The ESDIAD measurements are consistent with a model involving bonding of the undissociated  $H_2O$  molecule to the Ru substrate via the oxygen atom, and this suggestion will be discussed further in Section IV.

#### B. Low Energy Electron Diffraction

The clean Ru(001) surface exhibited a characteristic  $(1 \times 1)$  LEED pattern, and there were no new LEED structures observed during the adsorption of  $H_2O$  on Ru(001) at 90 K at any  $H_2O$  coverage. Adsorption of heavy doses of  $H_2O$  simply resulted in a decrease of intensity of the  $(1 \times 1)$  LEED beams and an increase in background intensity. The absence of an ordered LEED pattern at 90 K indicates that there is no long range order in the adsorbed layer, irrespective of the initial  $H_2O$  coverage.

For  $H_2O$  coverages of one monolayer or less, heating of the surface resulted in desorption of the adsorbate with the appearance of no LEED features other than the  $(1 \times 1)$  pattern characteristic of the clean surface. When the ice multilayer was formed at 90 K and heated, a weak, complex LEED pattern appeared at 120 K. This was apparently due to the thermally activated formation of a crystalline form of ice from the amorphous, as-deposited layer. Firment and Somorjai have also found evidence for ordered ice overlayers in LEED.<sup>(6)</sup> Further heating resulted in the development of a weak  $(2 \times 2)$  pattern. The persistence of the dim  $(2 \times 2)$  pattern following heating to  $< 1500$  K indicated that it was due to adsorbed atomic oxygen ( $\theta \sim 0.1$ ) resulting from dissociation of some of the adsorbed  $H_2O$ .

### C. Thermal Desorption Spectroscopy

Further evidence for the adsorption of undissociated water molecules, a small fraction of which dissociate as the surface is heated, is seen from thermal desorption studies. Upon heating the Ru(001) surface following exposure to  $H_2O$ , both  $H_2O$  and traces of  $H_2$  were observed as desorption products. Thermal desorption spectra of both products indicated multiple peak structures;  $H_2O$  desorbed from at least 3 binding states in the temperature range 100 to 500 K. The oxygen remaining on the surface following dissociation desorbs at  $\sim 1500$  K.

The thermal desorption spectra of  $H_2O$  shown in Figure 3 indicate a sequential filling of binding states as the  $H_2O$  coverage is increased. The most tightly bound state whose peak temperature  $T_p$  is at 230 K populates

first; the near constancy of  $T_p$  with increasing coverage is indicative of first order desorption kinetics. Assuming a pre-exponential factor of  $3 \times 10^{12}$ , the activation energy for desorption<sup>(7)</sup> of this state is calculated to be 12.6 kcal/mole. The fact that the state at  $T_p = 230$  K ceases to grow as the total  $H_2O$  coverage increases suggests that it is due to chemisorbed  $H_2O$  bonded to the metal surface in the first monolayer. The "halo" ESDIAD pattern of Fig. 1a is observed for  $H_2O$  coverages less than or equal to that of Fig. 3a, i.e.,  $\sim 0.20$  monolayers. The coverage which produces desorption spectrum 3b results in the hexagonal ESDIAD pattern of Fig. 1b, and for coverages corresponding to Fig. 3c or greater, the central spot pattern of Fig. 1c is seen. At higher coverages, the binding states having  $T_p$  values of 180 K and 200 K and corresponding to the onset of multilayer formation coalesce into a single state having  $T_p \sim 190$  K; this state simply grows in intensity as the coverage is increased, and evidently corresponds to desorption from a condensed ice multilayer. The shape of the peak at  $T_p = 190$  K is consistent with zero order desorption kinetics (rate of desorption independent of surface concentration, a situation which exists during free sublimation from the surface of a solid or liquid). The desorption rate increases exponentially with temperature on the leading edge, and drops precipitously as the multilayer is exhausted. Arrhenius plots based on the leading edges of a number of such desorption spectra (in which there were at least 4 monolayers of  $H_2O$  in the initial multilayer) yield an activation energy for desorption of 11.5 kcal/mole, in good agreement with the heat of sublimation of normal ice, 12.1 kcal/mole.

Further evidence that the peak at  $T_p = 230$  K corresponds to the chemisorbed  $H_2O$  monolayer in direct contact with the Ru(001) substrate

is seen by comparing Figures 3 and 4. Preadsorption of a monolayer of oxygen (20L  $O_2$  exposure at  $\sim 90$  K, heat to 600 K, cool to 90 K before exposure to  $H_2O$  vapor) effectively "blocks" adsorption of  $H_2O$  into this state. Desorption from the condensed  $H_2O$  multilayer state(s) however, is virtually unaffected by the nature of the adsorbed monolayer.

Finally, it should be noted that both the  $H_2$  and  $H_2O$  desorption spectra were sensitive to traces of impurities present on the surface during the thermal cleaning process.

#### IV. DISCUSSION

##### A. Adsorption of $H_2O$ in the First Monolayer

The initial interaction between a water molecule and the surface of a transition metal is expected to be via the non-bonding (or "lone pair")  $b_1$  and  $a_1$  orbitals<sup>(3)</sup> located primarily on the oxygen end of the molecule. (By analogy, the hydration of most metal ions occurs via bonding of the metal ion to the oxygen end of several water molecules). In the adsorption of  $H_2O$  on Ru, dative bonding can occur between the water lone pair orbitals and the Ru d orbitals. For weak bonding of  $H_2O$  to Ru, little distortion of the HOH bond angle is expected. Although no UPS data for  $H_2O$  on Ru are available, Brundle and Carley<sup>(8)</sup> have examined the adsorption of a fractional monolayer of  $H_2O$  on a Ni film at 77 K. Their results demonstrate that there are only small differences between the orbital structure of adsorbed  $H_2O$  and gaseous  $H_2O$ , suggesting little distortion of the undissociated  $H_2O$  molecule upon adsorption. In addition, McCarty and Madix<sup>(9)</sup> used thermal desorption spectroscopy to show that  $H_2O$  is molecularly adsorbed on clean and carburized Ni(110). Finally, for adsorption of  $H_2O$  on Ru(001), the present thermal desorption studies show that  $H_2O$  is molecularly



adsorbed in the first monolayer on a Ru(001) surface at 90 K.

A model of  $\text{H}_2\text{O}$  adsorption on Ru(001) consistent with the experimental results is shown in Fig. 5. The "halo" ESDIAD pattern of Fig. 1a is envisioned to arise from ESD of  $\text{H}^+$  ions from  $\text{H}_2\text{O}$  at low coverages ( $\sim 0.2$  monolayers); interactions between neighboring water molecules are weak, and the azimuthal orientations of the molecules are random and non-coordinated. Rotational freedom about the  $\text{C}_{2v}$  axis may exist. The statistical average of  $\text{H}^+$  ions produced by ESD of the random array of  $\text{H}_2\text{O}$  molecules gives rise to the observed halo. Further evidence for the proposed structure is found in the measurement of the  $\text{H}^+$  ion desorption angles. The cone angle of the region of maximum intensity of the halo is  $116 \pm 10^\circ$ , in comparison with the  $104.5^\circ$  angle of the free molecule.

Clinton<sup>(10)</sup> has shown that upon excitation of a ligand to a repulsive ionic state in a spherically symmetric force field, the initial impulsive force leading to ionic desorption should be in the same direction as the initial bond angle. In the case of adsorbed  $\text{H}_2\text{O}$ , at least two other factors could influence the observed ion trajectory: the deviation of the initial bond angle from that of the free  $\text{H}_2\text{O}$  molecule due to the bonding interaction, and the influence of the image field as the  $\text{H}^+$  ion desorbs. Charge transfer from the  $\text{H}_2\text{O}$  molecule to the Ru substrate would be expected to increase the HOH bond angle (e.g., the HOH angle in free  $\text{H}_2\text{O}^+$  is  $110.6^\circ$ <sup>(11)</sup>). In addition, the effect of the attractive image field on the desorbing  $\text{H}^+$  ion will also increase the apparent ion desorption angle; the magnitude of this effect depends on the ion kinetic energy, the bond angle, and the distance between the ionized ligand and the image plane. The fact that the experimentally determined ion desorption angle is larger

than the free molecule value is an indication that perturbations of the HOH bond angle and of the ion trajectory do occur.

At higher  $\text{H}_2\text{O}$  coverages ( $>0.2$  monolayers), a hexagonal array of  $\text{H}^+$  emission cones is seen in the ESDIAD pattern (Fig. 1b). In this coverage range, lateral interactions between neighboring  $\text{H}_2\text{O}$  molecules apparently result in the formation of domains in which the orientations of the  $\text{H}_2\text{O}$  molecules are coordinated due to the symmetry of the substrate. One such array which could give rise to the observed ESDIAD pattern is shown in the central panels of Fig. 5. Note that no ordered LEED pattern other than the  $(1 \times 1)$  pattern characteristic of the clean substrate was seen during  $\text{H}_2\text{O}$  adsorption at 90 K, so that if ordered domains having other symmetry exist, they can have only short range order ( $< 15 \text{ \AA}$  (12)). Finally, if we assume that the O atoms are bonded to single Ru atoms, the coincidence of the  $\text{H}^+$  ESDIAD hexagon with respect to the substrate atom array (Fig. 1a, 1c) suggests that the azimuthal orientations of the H atoms in adsorbed  $\text{H}_2\text{O}$  are in the direction of nearest neighbor surface atoms. (As discussed in III-A, the LEED hexagon is rotated by  $30^\circ$  from the substrate atom hexagonal array.)

Although the model described above is by no means unequivocal, it does demonstrate a unique feature of ESDIAD and its relationship to surface structure. In a number of cases, coherent ESDIAD patterns have been seen from overlayers in which long range order appears to be absent. A coherent ESDIAD pattern requires only that the molecules which yield ion emission be bonded in geometrically similar sites. There is no requirement of translational order, either long or short range. In addition, ESDIAD provides information about the locations of H atoms in molecules, information often unavailable in LEED studies in which scattering is dominated by ligands containing heavier adatoms. (13)



## B. Multilayer formation

ESDIAD of the ice multilayer reveals that  $H^+$  ions desorbing normal to the surface are the dominant desorption products with fragments identified as  $H_2^+$ ,  $O^+$ ,  $OH^+$ ,  $H_2O^+$  and  $(H_3O)^+$  seen at the 1% level. This is in contrast to ESD of multilayers of  $C_6H_{12}$  and  $C_8H_{16}$  in which the ion desorption mass spectra closely resembled the gas phase ionization "cracking patterns".<sup>(14)</sup> In the condensed hydrocarbons, the bonding is largely of the van der Waals type whereas the formation of hydrogen bonds dominate the bonding in ice. The existence of strong intramolecular bonding in ice presumably affects the ionization and ion reneutralization processes in ESD, leading to a high yield of  $H^+$  compared to gas phase electron impact ionization.

A question which has received much attention in the ice literature concerns the orientation of  $H_2O$  molecules in the surface layer of water and ice; i.e., does the H or the O end of the molecule point away from the surface? Fletcher<sup>(15)</sup> has written extensively on this topic; his current thinking is that the low energy configuration is that in which surface molecules have their protons buried in the liquid. The ESDIAD observation of an intense beam of  $H^+$  ions normal to the surface indicates that the OH bonds point outward from thick layer of vitreous ice formed at 77 K (right panel of Fig. 5).

Finally, we note that verification of these conclusions concerning the conformation of adsorbed  $H_2O$  should be accomplished using an independent technique (e.g., Angular resolved ultraviolet photoemission spectroscopy) in order to more completely evaluate the utility of ESDIAD in surface structure determination.

## V. ACKNOWLEDGEMENTS

The authors acknowledge with pleasure valuable discussions with Dr. D. Wayne Goodman of NBS and Prof. Paul Camp, U. of Maine. This work was supported in part by the Office of Naval Research.

# REFERENCES

- 1) T. E. Madey and J. T. Yates, Jr., Surface Science 63, (1977).
- 2) T. E. Madey, J. J. Czyzewski and J. T. Yates, Jr., Surface Science 57, 580 (1976); Surface Science 49 465 (1975).
- 3) J.H.D. Eland, "Photoelectron Spectroscopy", (Butterworths, London, 1974).
- 4) D. Eisenberg and W. Kauzmann, "The Structure and Properties of Water", (Oxford University Press, New York and Oxford, 1969).
- 5) T. E. Madey, H. A. Engelhardt, and D. Menzel, Surface Science 48, 304 (1975); T. E. Madey and D. Menzel, Japan J. Appl. Phys. Suppl. 2, Pt. 2, p. 229 (1974).
- 6) L. E. Firment and G. A. Somorjai, Surface Science 55, 413 (1976).
- 7) P. A. Redhead, Vacuum 12, 203 (1962).
- 8) C. R. Brundle and A. F. Carley, Faraday Discussions of the Chem. Soc. 60, 51 (1975).
- 9) J. G. McCarty and R. J. Madix, Surface Science 54, 121 (1976).
- 10) W. Clinton, Phys. Rev. Letters, submitted for publication.
- 11) H. Lew and I. Heiber, J. Chem. Phys. 58, 1246 (1973).
- 12) G.-C. Wang, T.-M. Lu, and M. G. Lagally, Bulletin of the Am. Phys. Soc. 22, 356 (1977).
- 13) L. L. Kesmodel and G. A. Somorjai, Bulletin of the Am. Phys. Soc. 22, 355 (1977).
- 14) T. E. Madey and J. T. Yates, Jr., to be published.
- 15) N. H. Fletcher, in E. Whalley, S. J. Jones and L. W. Gold, eds., "Physics and Chemistry of Ice" (Royal Society of Canada, Ottawa, 1973) p. 132; N. H. Fletcher, "The Chemical Physics of Ice" (Cambridge University Press, 1970) p. 126.

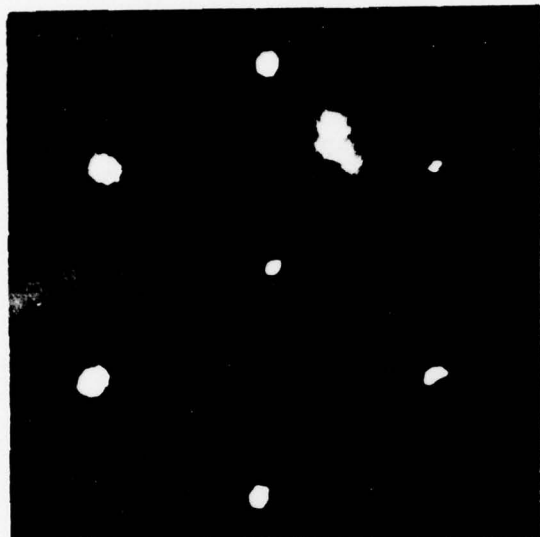
# FIGURE CAPTIONS

- Fig. 1. LEED and ESDIAD patterns for  $H_2O$  on Ru(001). (a) LEED of clean surface, electron energy  $V_e = 200$  eV; bias potential between crystal and first grid of detection system<sup>(1)</sup>  $V_B = 100$  V. (b) -(d),  $H^+$  ESDIAD patterns. (b)  $H_2O$  coverage  $\theta < 0.2$ ,  $V_e = 200$  eV,  $V_B = 100$  V. (c)  $\theta \sim 0.2$ ,  $V_e = 300$  eV,  $V_B = 200$  V. (d)  $\theta > 1$  (ice multilayer)  $V_e = 200$  eV,  $V_B = 100$  V.
- Fig. 2. ESDIAD of  $H_2O$  adsorbed on Ru(001) at  $\sim 90$  K. Apparent value of  $H^+$  emission cone half angle,  $\alpha$ , plotted vs. the potential  $V_B$  between the crystal and the first hemispherical grid of the detection system. The inset drawing defines  $\alpha$ .
- Fig. 3. Thermal Desorption Spectra for desorption of  $H_2O$  from Ru(001).
- Fig. 4. Thermal Desorption Spectra demonstrating the influence of preadsorbed oxygen on the bonding of  $H_2O$  to Ru(001). Note that preadsorbed oxygen blocks the  $H_2O$  peak at  $T_p = 230$  K.
- Fig. 5. Proposed models of  $H_2O$  adsorption based on ESDIAD patterns of Fig. 1.



# ESDIAD

## Adsorption of $\text{H}_2\text{O}$ on $\text{Ru}(001)$



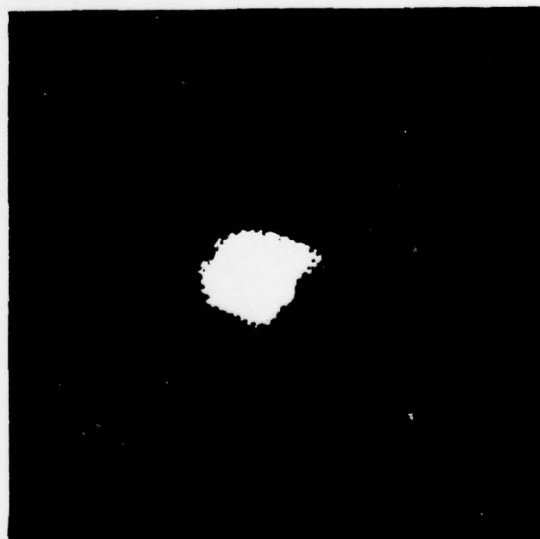
(a) clean  $\text{Ru}(001)$  LEED



(b)  $\theta < 0.2$

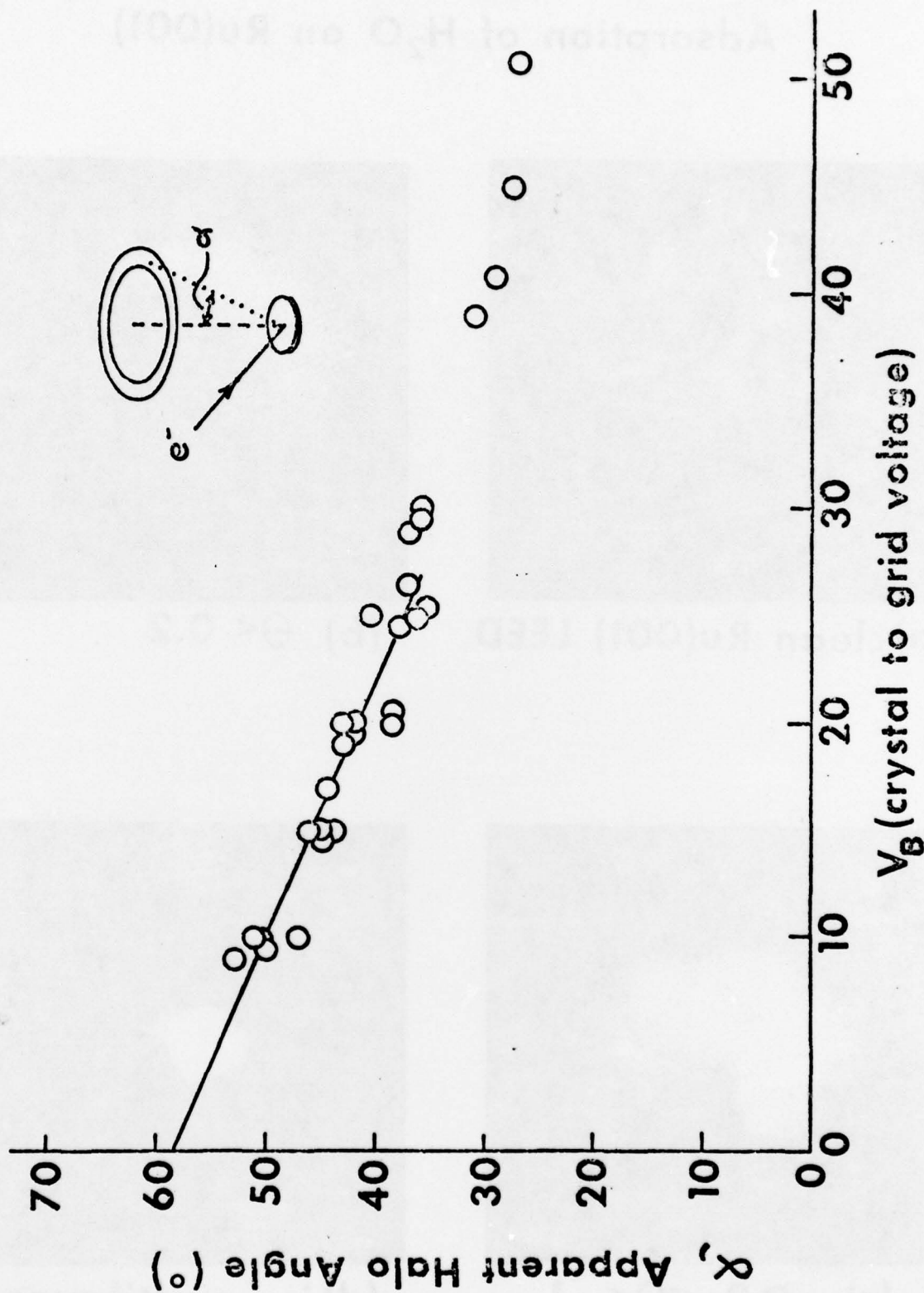


(c)  $0.2 < \theta < 1$



(d) ice multilayer

# ESDIAD of $H^+$ from $H_2O$ Adsorbed on $Ru(001)$





# THERMAL DESORPTION OF $\text{H}_2\text{O}$ FROM $\text{Ru}(001)$

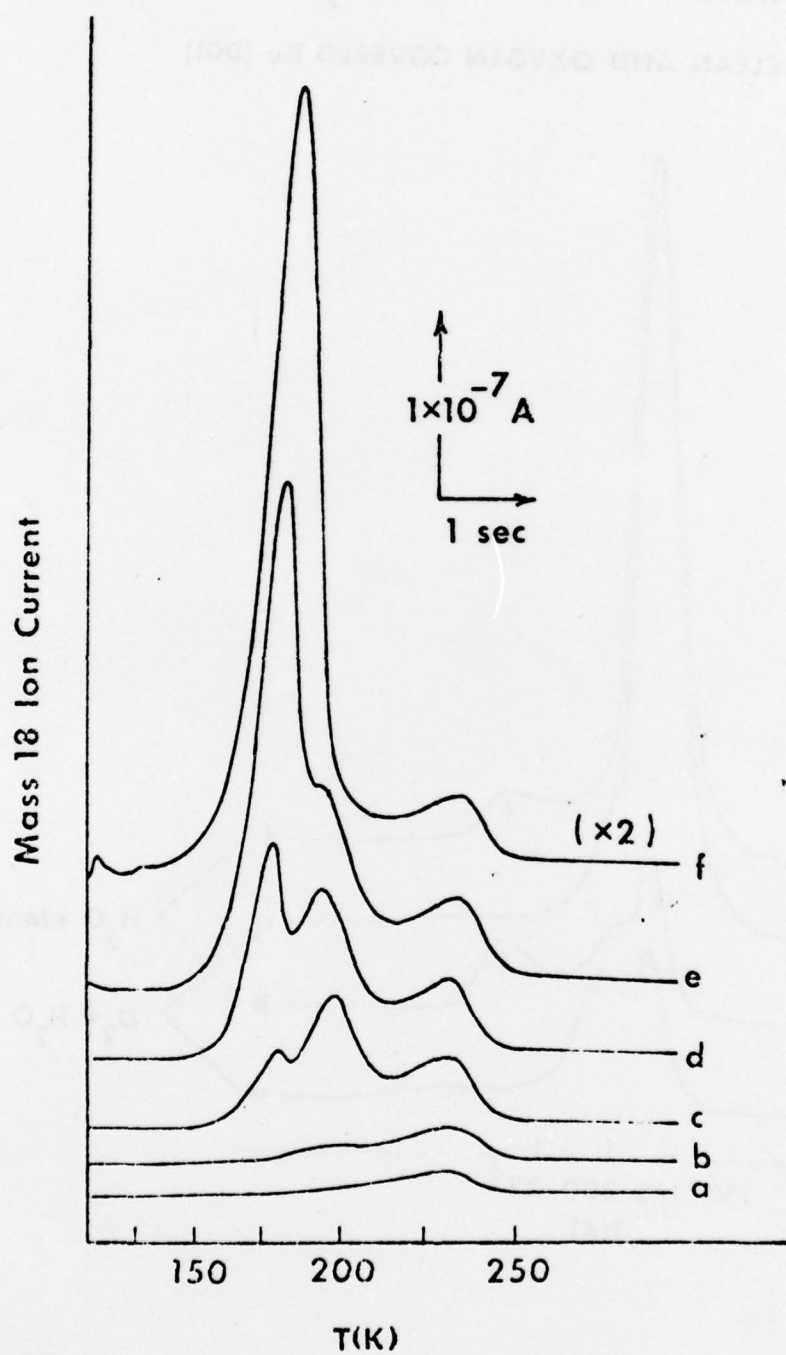


FIG. 3

THE THERMAL DESORPTION OF H<sub>2</sub>O FROM  
CLEAN AND OXYGEN COVERED Ru (001)

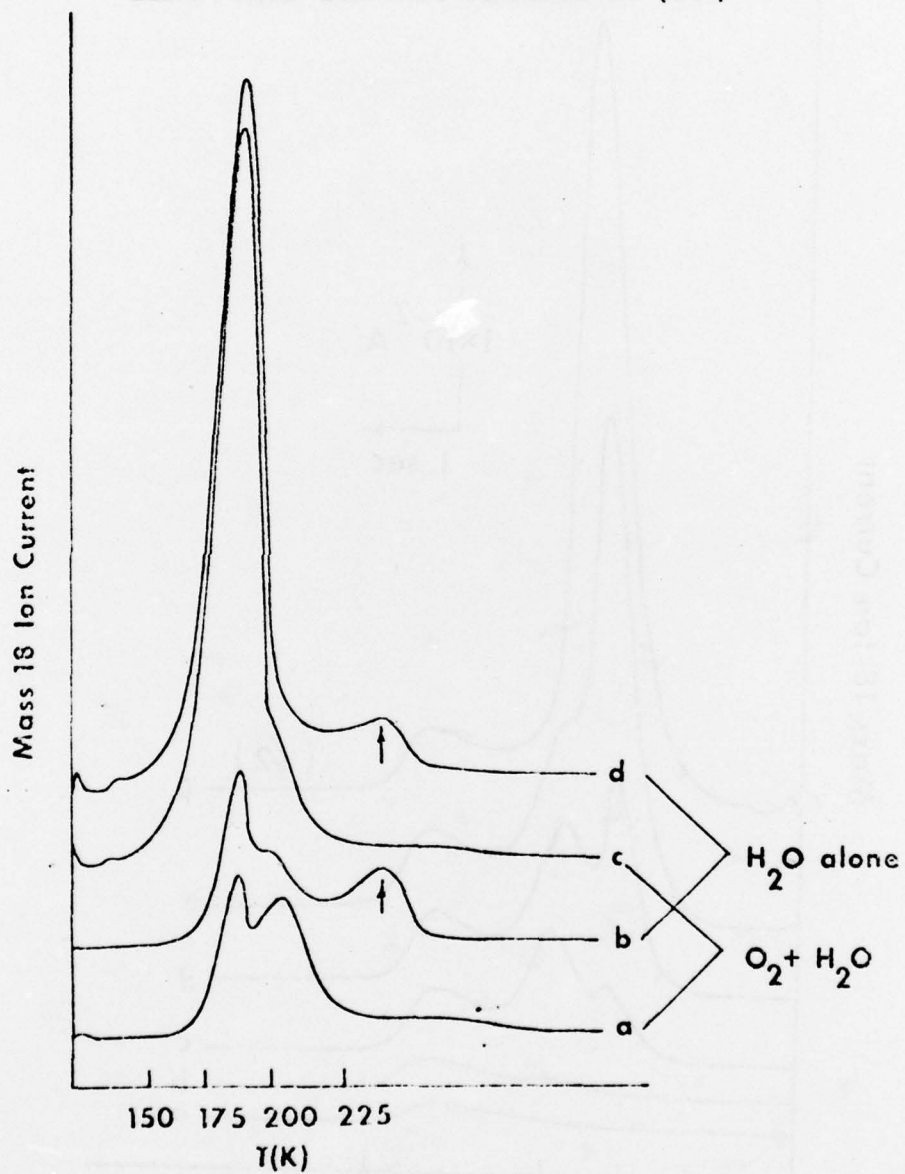
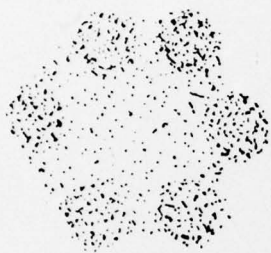
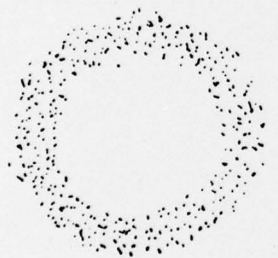


FIG. 4

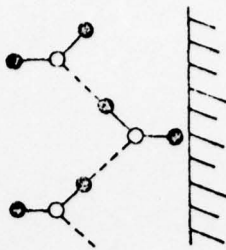
# ESDIAD of H<sub>2</sub>O on Ru(001)

ESDIAD patterns



Proposed structures

side view



top view

